Evolution of Asian Aerosols during Transpacific Transport in INTEX-B

Edward J. Dunlea[1], Peter F. DeCarlo[1,2,*], Allison C. Aiken[1,3], Joel R. Kimmel[1], Richard E. Peltier[4,**], Rodney J. Weber[4], Jason Tomlinson[5,***], Don R. Collins[5], Yohei Shinozuka[6], Cameron S. McNaughton[6], Steven G. Howell[6], Anthony D. Clarke[6], Louisa K. Emmons[7], Eric C. Apel[7], Gabriele G. Pfister[7], Aaron van Donkelaar[8], Randall V. Martin[8,9], Dylan B. Millet[10], Colette L. Heald[11,****] and Jose L. Jimenez[1,3]

(Supplemental Information)

Final Version for Atmospheric Chemistry and Physics

Section S.1 – C-130 Aerosol Instrument Intercomparisons with other aircraft

Two intercomparisons of the C-130 and DC-8 were performed, one on 4/17/2006 and one on 5/15/2006. The two planes flew side-by-side in a linear flight pattern for a total between the two flights of more than 2 hours of flight time covering the altitude range between 1,000 and 20,000 ft. The DC-8 had two measurements of aerosol composition on board: a mist chamber (Cofer, et al., 1985) with a size cutoff ~ 1 μm and bulk aerosol filters with a size cutoff ~ 4.5 μm. Time series plots of the C-130 aerosol measurements during these intercomparison periods reveal relatively good agreement amongst all instruments for the inorganic aerosol mass measurements. Again, all data have been converted to STP as above. Supplemental Table S1 lists the average sulfate concentrations by all instruments for each of the three altitudes. Supplemental Figure S2 shows an example comparison for sulfate on 5/15/2006, which shows the typical level of agreement for these intercomparisons under these low ambient concentration conditions. Note a plume of sulfate near 7:05 PM, which is apparent in the nephelometer data but is only captured by the AMS due to its higher time resolution. The subsequent plume in the nephelometer data is not reflected in any of the other instruments; there was no indication of dust during this time. We note that NASA frequently performs blind measurement intercomparisons throughout field experiments to assess data quality. During these measurement periods investigators submit data in the field to an independent reviewer without investigator access to other data. During this study the PILS and DC-8 instruments submitted data to these intercomparisons. The AMS was not able to participate in these field intercomparisons as it was a new instrument, and its calibration and data analysis software were still under development during and after the field campaign. For the intercomparisons reported here the analysis was performed after all data had been submitted.

<u>Section S.2 – Organic Aerosol Mass Spectra</u>

In addition to organic aerosol formation, we can further examine the oxidation state of the organic aerosol with the AMS mass spectra (Alfarra, et al., 2004; Zhang, et al., 2007; Zhang, et al., 2005c). Supplemental Figure S7 shows the high resolution mass spectra of the two Asian pollution layers, where the organic aerosol in both cases is highly oxidized, showing a much larger contribution from the fragment ions containing carbon, hydrogen and oxygen ($C_xH_yO_z^+$) compared to fragment ions containing only carbon and hydrogen ($C_xH_y^+$). However, comparing the mass spectra from the older Asian layer (7-10 days) with the younger Asian layer (3-4 days) shows that the older layer is indeed more oxidized, showing a relative increase in two major $C_xH_yO_z^+$ fragment ions (CHO^+ and CO_2^+), while showing a relative decrease in many of the $C_xH_y^+$ fragment ions. This is consistent with increased aging of the OA during the relative elapsed time between layers determined earlier from meteorological and tracer considerations.

Supplemental Figure S12 shows selected ions from high-resolution mass spectra for the various air mass types discussed in Section 3; we see that the highest organic fragment ion peak is *m/z* 44, CO_2^+, indicative of highly processed aerosol (Alfarra, et al., 2004; Mohr, et al., 2009; Zhang, et al., 2005a; Zhang, et al., 2005c). Analyzing the different ions at the same nominal mass-to-charge ratios, such as those at *m/z* 43, 55 and 57, the overall trend is that $C_xH_yO_z^+$ fragment ions are typically larger than $C_xH_y^+$ fragment ions for all air mass types. If we use the ratio of the $C_2H_3O^+$ and $C_3H_7^+$ peaks at nominal *m/z* 43 as a gauge since this mass tends to be most representative of the bulk OA (Mohr, et al., 2009; Zhang, et al., 2004), we estimate that the organic aerosol from the Asian pollution and free tropospheric air mass types is roughly three times as oxidized as that from the Central Valley and Seattle region air mass types, which is consistent with the Central Valley and Seattle region aerosol being closer to urban pollution centers. The inorganic ions show the typical lack of significant interferences for unit mass resolution *m/z* 48 and 64 for the determination of sulfate (Jimenez, et al., 2003), as well as illustrating the interferences that make the determination of NH_4^+ from unit mass resolution spectra more challenging and noisy (Allan, et al., 2004).

Table S1 – Average sulfate concentrations measured during C-130 and DC-8 intercomparison flight on 5/12/2006 divided up for the three level flight legs of the intercomparison time period. Uncertainties for are the combination of 1 sigma standard deviation of the average during the time period and instrument uncertainty.

Measurement	Alt 1 (18 kft)	Alt 2 (5.5 kft)	Alt 3 (1 kft)
AMS SO4	0.28 ± 0.08	0.49 ± 0.14	0.68 ± 0.22
Filter SO4	0.12 ± 0.09	0.35 ± 0.10	1.11 ± 0.22
MC Fine SO4	0.17 ± 0.08	0.26 ± 0.08	0.86 ± 0.23
PILS SO4	0.30 ± 0.10	0.35 ± 0.12	1.02 ± 0.31

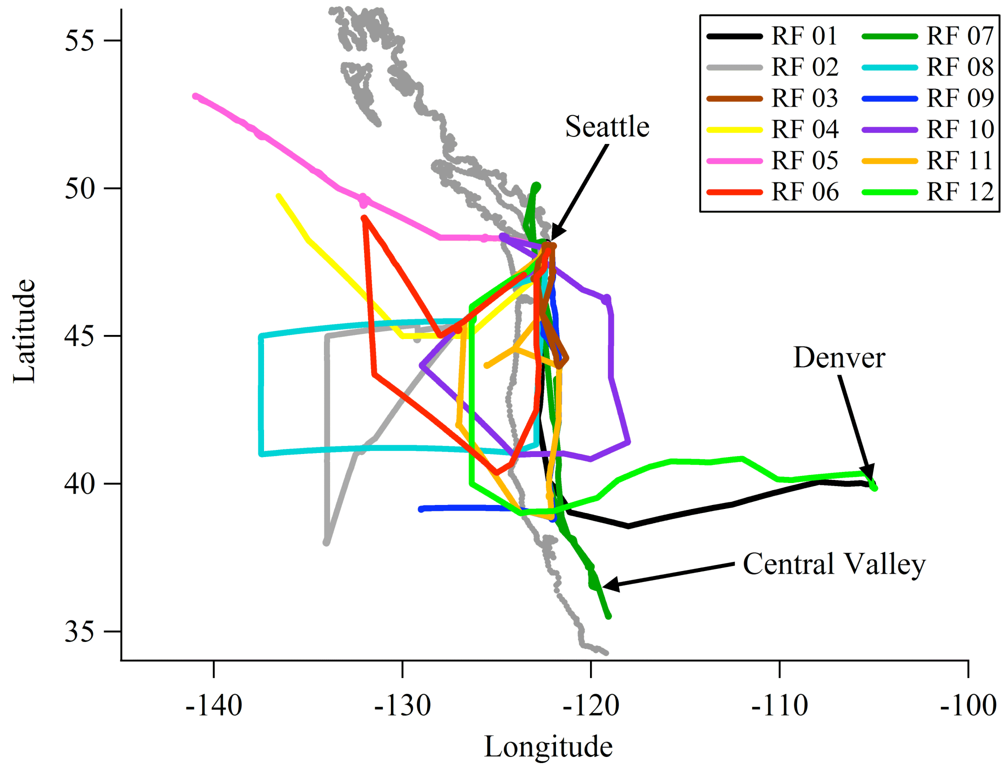

74

75 Figure S1 – Map of C-130 flight tracks during INTEX-B campaign.

76

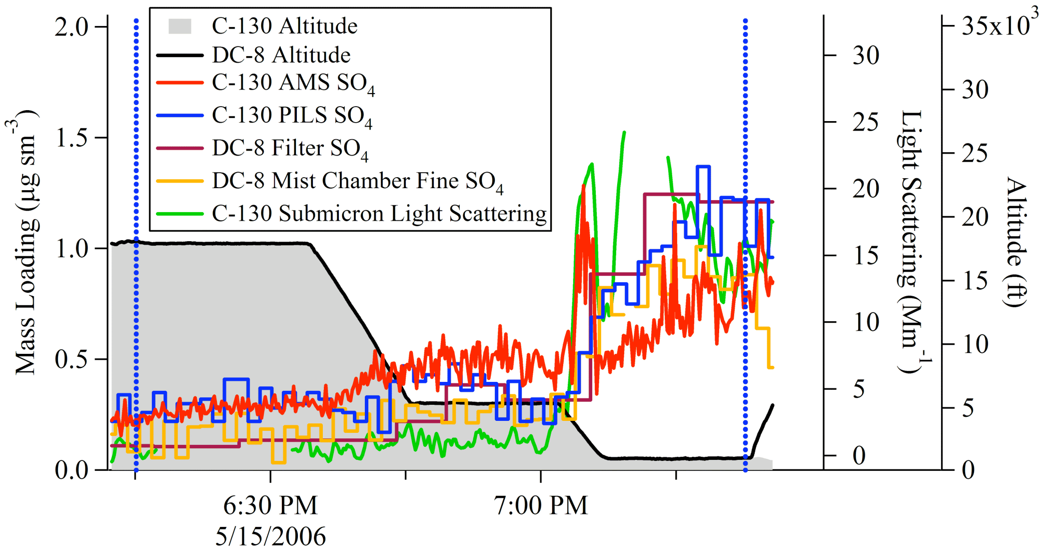

Figure S2 – Example time series plot from one of the two intercomparison flights on 5/15/2006. Measurements of sulfate from various instruments on board the C-130 and DC-8 aircrafts are shown (see text for description of instruments) along with the altitude of the C-130; the DC-8 altitude closely matched that of the C-130. The dashed vertical lines denote the start and end times of the intercomparison. The time is in UTC. In general, the agreement of the various sulfate measurements is relatively good.

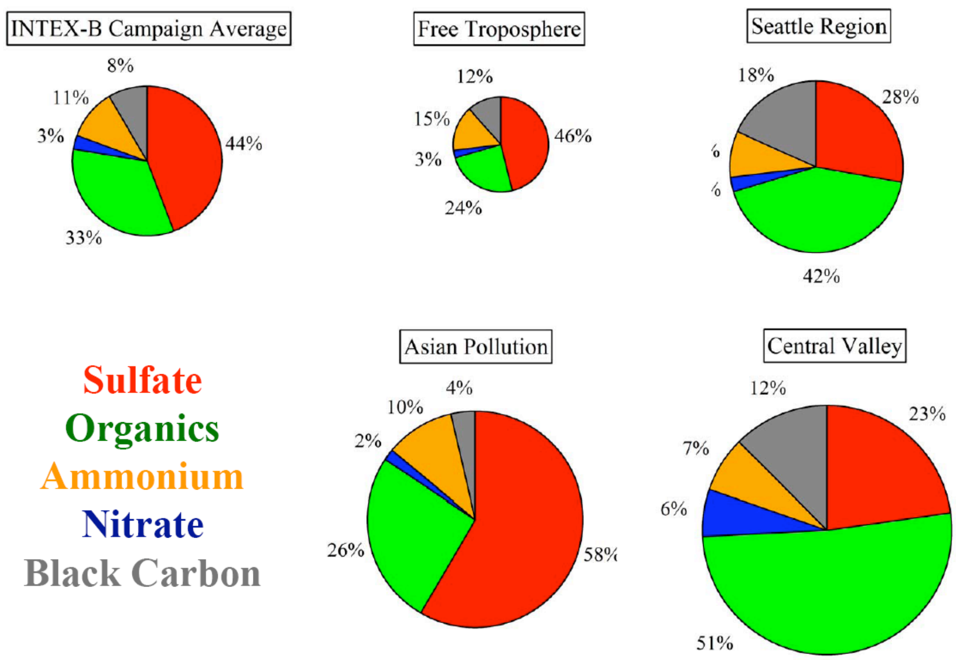

Figure S3 – Pie charts of average relative concentrations of submicron aerosol as measured by AMS and SP2 for overall INTEX-B campaign average and various air mass types as defined in Section 3. Area of pie charts is proportional to the average total concentration of that air mass category. Concentration values are listed in Table 3.

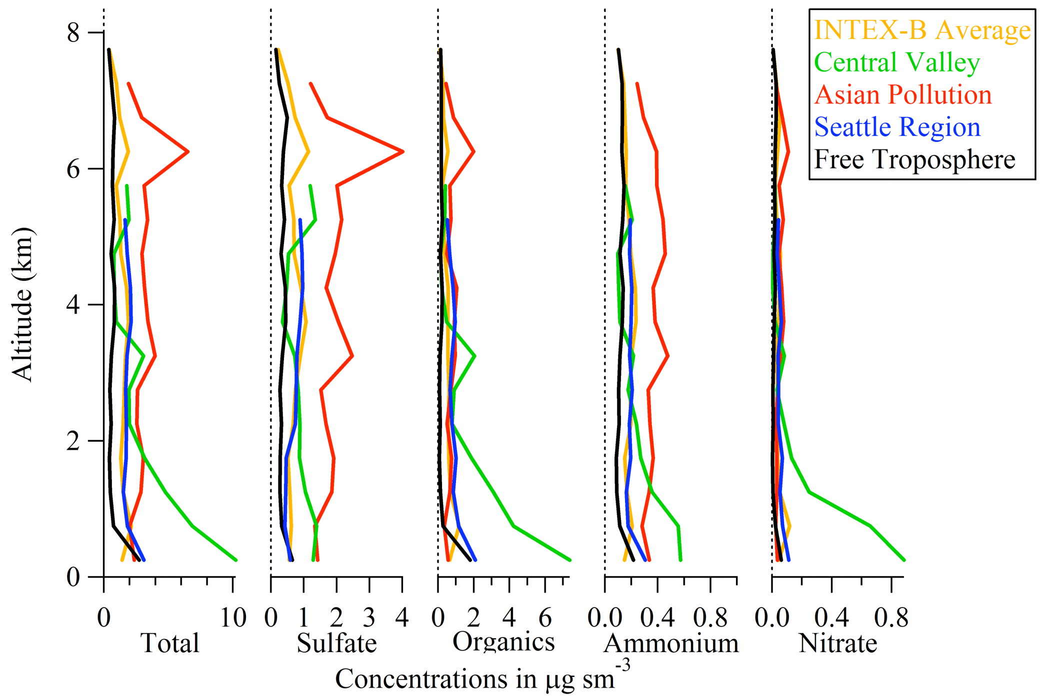

Figure S4 – Average vertical profiles for various types of air masses; see text for definitions of air mass types. The dashed lines are zero lines for the various species.

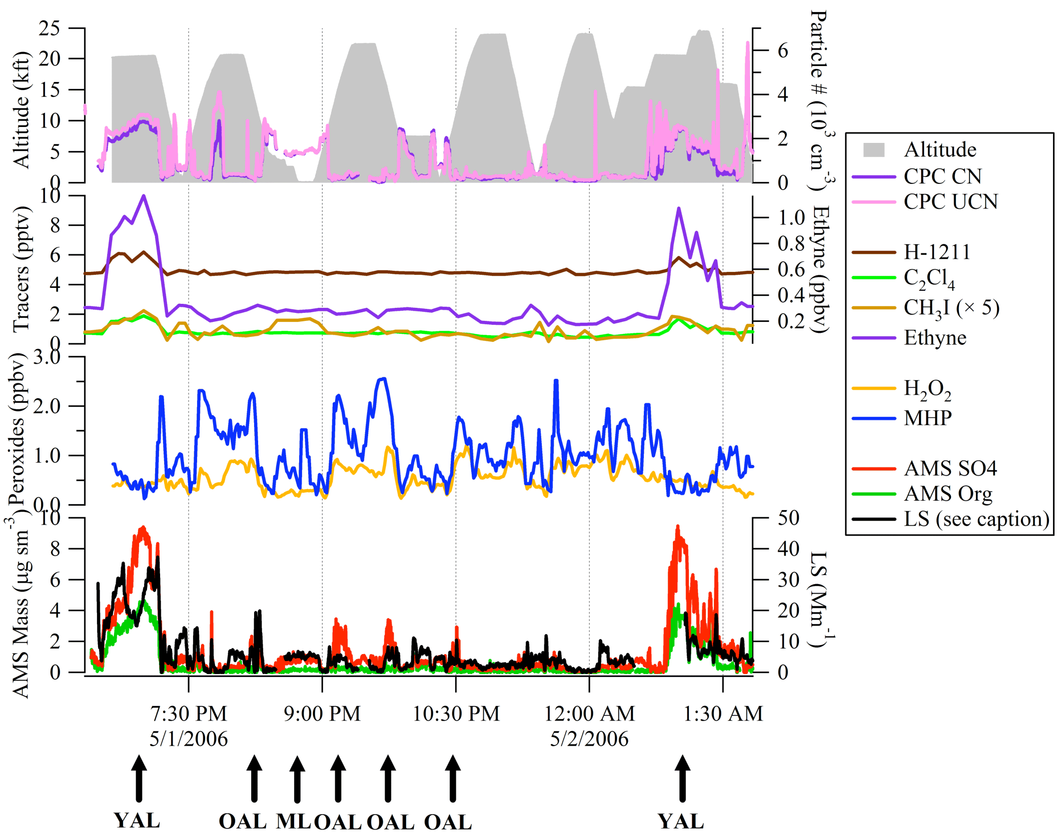

Figure S5 – Time series of additional measured species during the 5/1/2006 research flight, which are not displayed in Figure 5. Again, two intercepts of the Younger Asian Layer (YAL), several intercepts of the Older Asian Layer (OAL) and the one Marine Layer (ML) that are discussed in the text are labeled. LS is an abbreviation for submicron light scattering from the nephelometer instrument; CN is condensation nuclei and UCN is ultrafine condensation nuclei; time is in UTC.

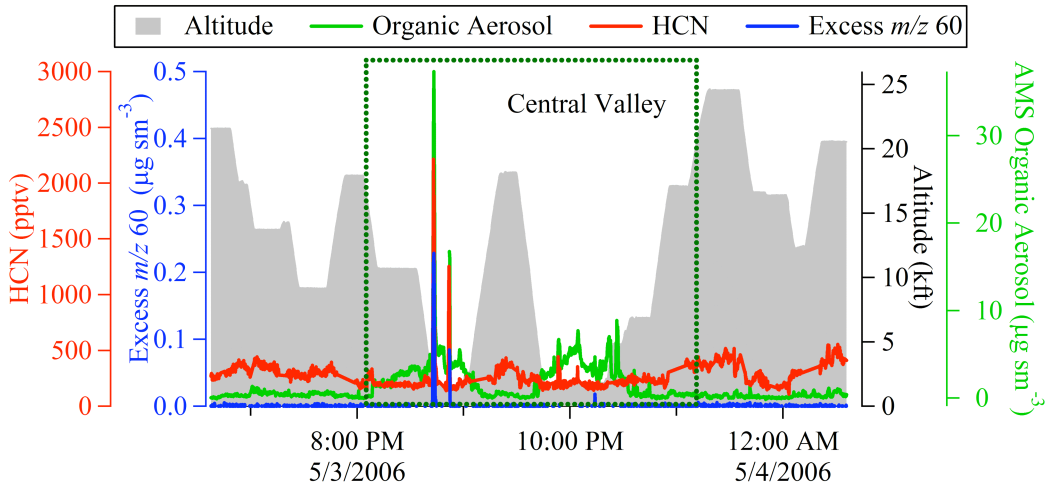

Figure S6 – Time series of biomass burning markers and organic aerosol during research flight 07 (5/3/2006), where the time period defined as the Central Valley is designated by the dashed green box. Both gas phase HCN and aerosol phase organic aerosol signal at *m/z* 60 are indicative of biomass burning. Excess m/z 60 is defined as (m/z 60 – 0.3% * total organics) in order to isolate the portion due to biomass burning (DeCarlo, et al., 2008).The influence of biomass burning during the Central Valley time period (Section 3.2) is apparent in only two very short duration plumes and is minimal overall for the Central Valley air mass.

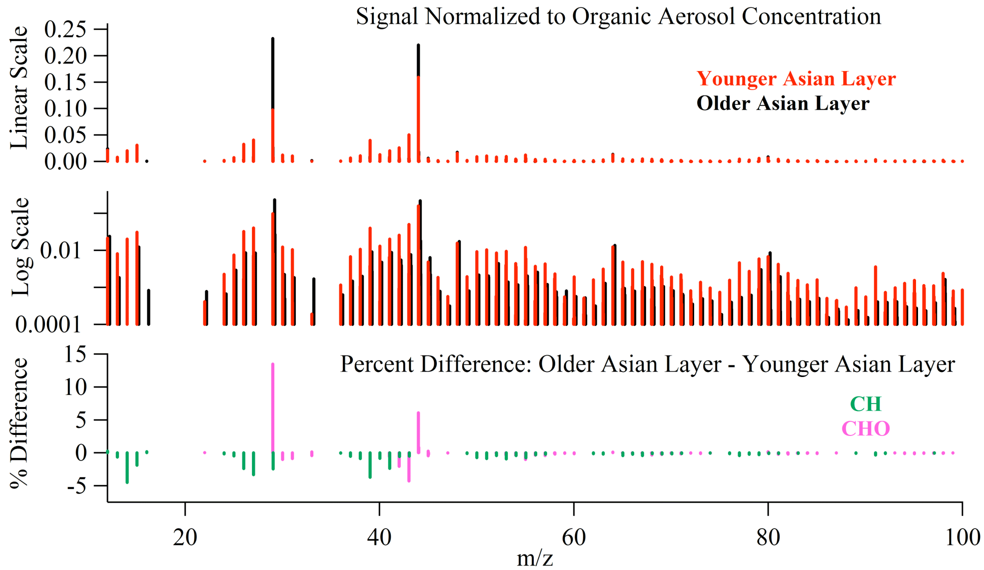

Figure S7 –Upper two panels show the high resolution mass spectra recorded with AMS for younger Asian layer (Section 3.1.1) and older Asian layer (Section 3.1.2), on both a linear and log scale. Inorganic peaks have been removed from plot. Signals are normalized to the total organic aerosol loading during the individual time periods. The bottom panel shows the difference between the two normalized spectra from the upper panel highlighting the increase in oxygen containing fragment ions (CHO) and the decrease in fragment ions containing only carbon and hydrogen (CH) in the older Asian layer. The younger Asian layer has 5% of the organic mass contained in fragment ion peaks larger than 100 amu, where the older Asian layer has 2%.

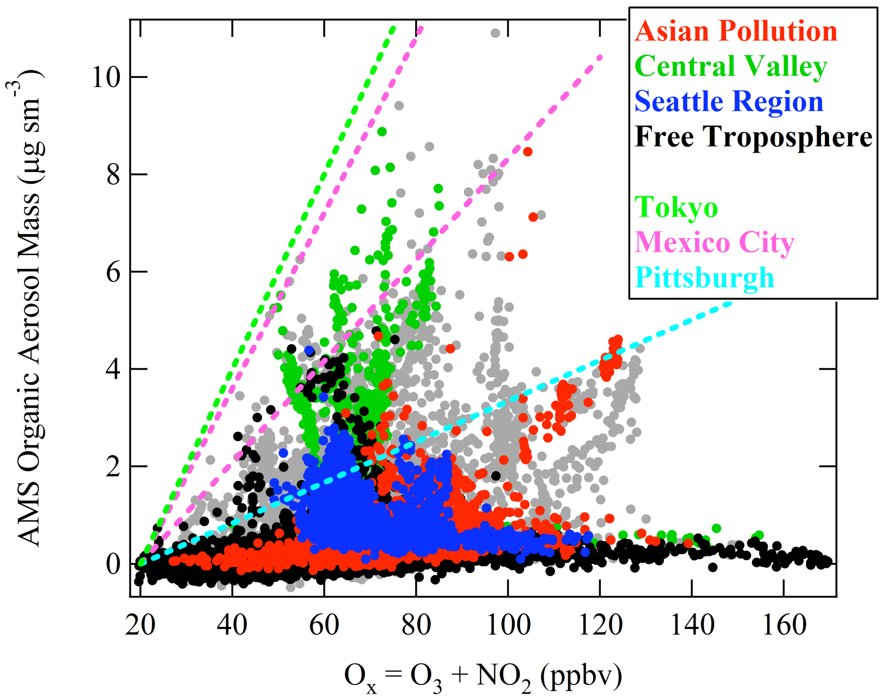

Figure S8 – Comparison of measured organic aerosol mass from the AMS on board the C-130 with the measured O_x, defined as the sum of $O_3 + NO_2$. Unclassified points are in gray. Dashed pink lines represent ratios of OA/O_x from Mexico City (Herndon, et al., 2008) of (104-180) µg sm^{-3} ppmv^{-1}; dashed light green line represents ratio of 200 µg sm^{-3} ppmv^{-1} from Tokyo (Kondo, et al., 2008); dashed cyan line represents the ratio from Pittsburgh (Zhang, et al., 2005b) 38 µg m^{-3} ppmv^{-1} (adjusted by 10% to account for STP).

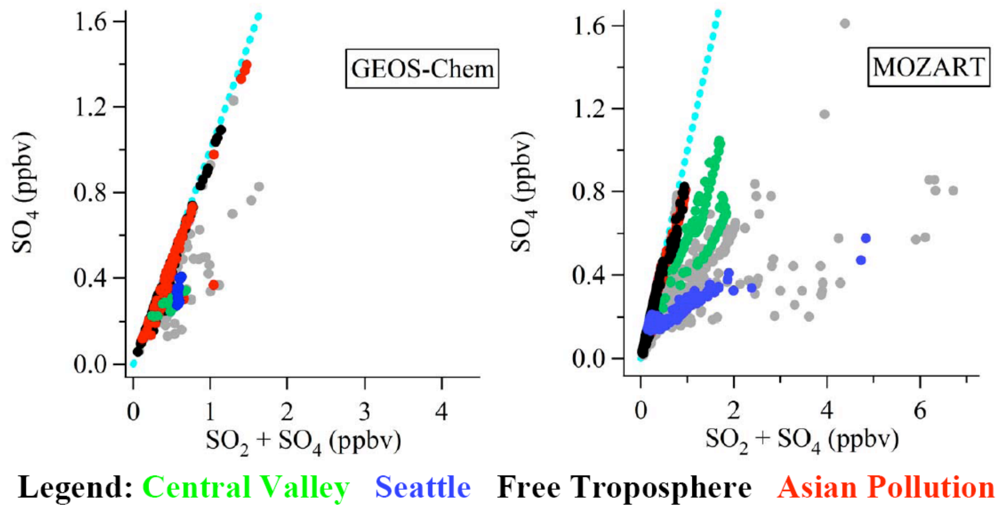

Figure S9 – Scatter plots of modeled aerosol sulfate levels converted to equivalent gas phase ppbv versus the total sulfur from the modeled aerosol sulfate plus the gas phase SO_2 from GEOS-Chem (left panel) and MOZART (right panel). The dashed lines indicate the 1:1 line where all sulfur is aerosol sulfate. Unclassified points are in gray.

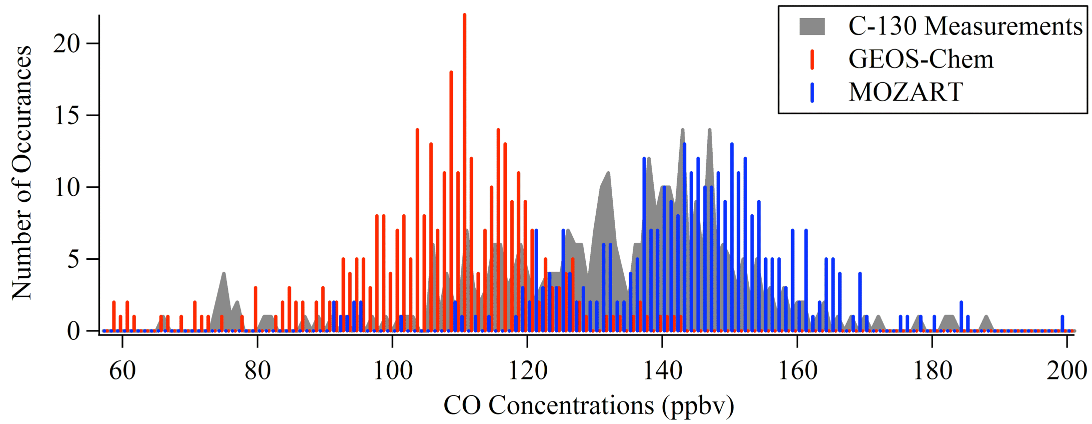

Figure S10 – Histograms of CO values from C-130 measurements, GEOS-Chem and MOZART modeled products for the entire INTEX-B campaign.

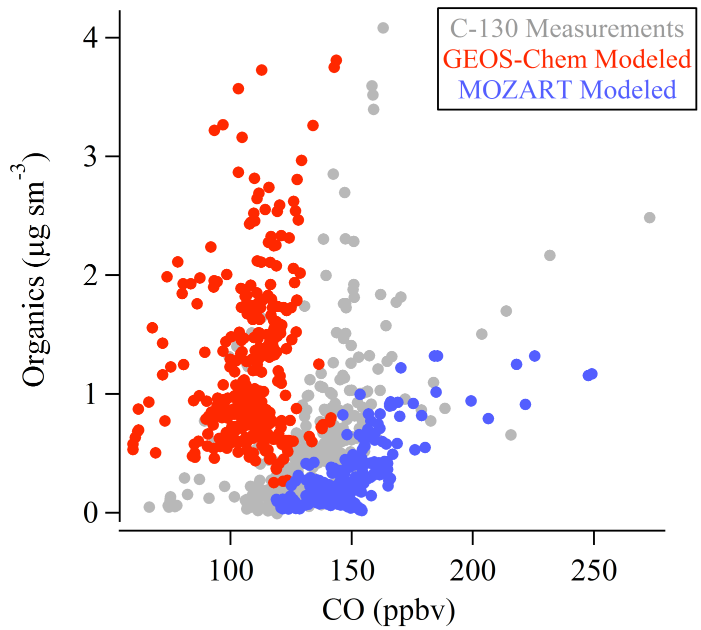

Figure S11 – Scatter plot of organic aerosol mass versus gas phase CO for measurements from the C-130 and chemical transport models for the entire INTEX-B campaign (15 minute time base).

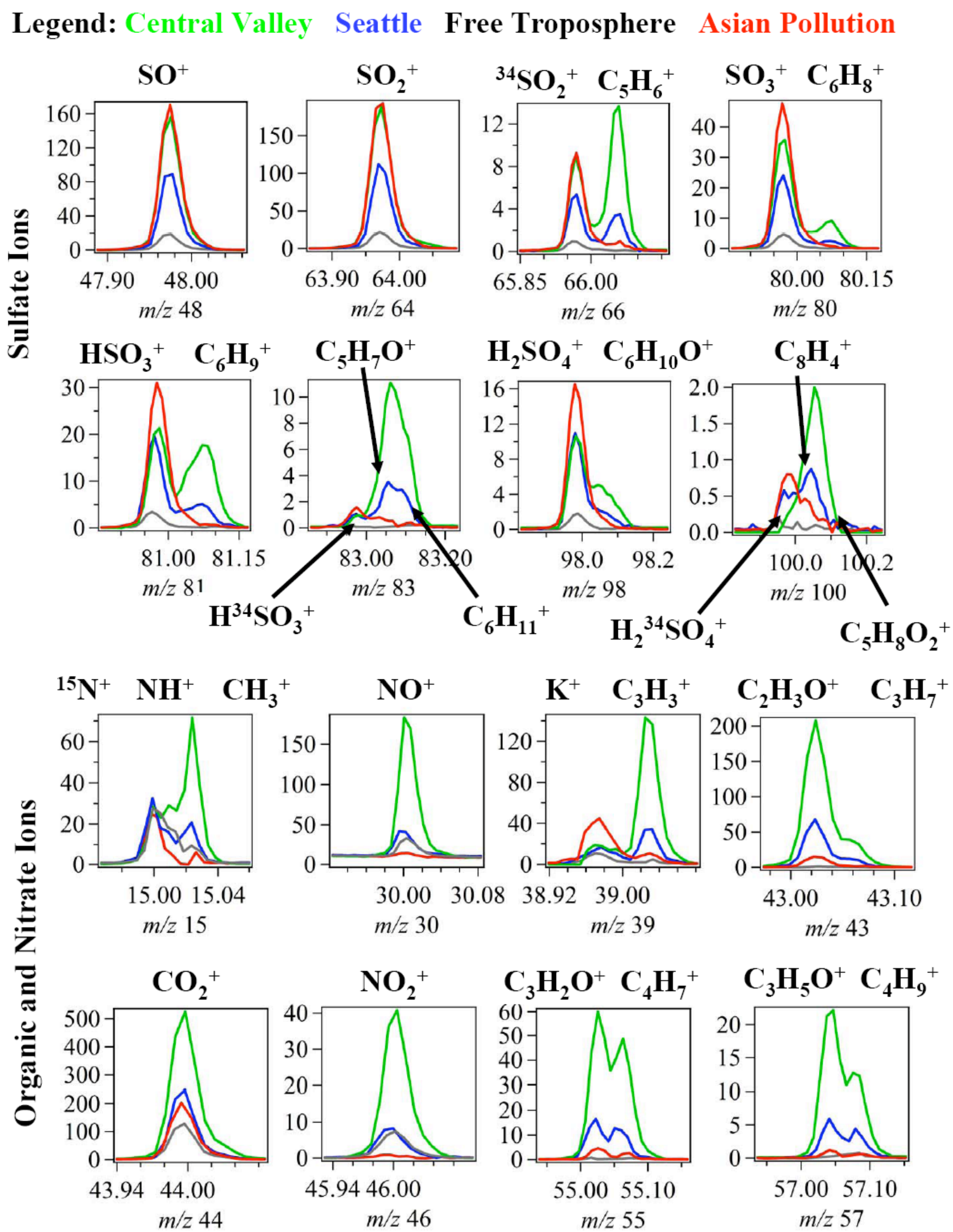

Figure S12 – Example peaks in high resolution mass spectra for the various air mass types described in the text. The peak shape for K^+ ions is wider because K^+ is emitted from the vaporizer within the AMS.

References

Alfarra, M.R., Coe, H., Allan, J.D., Bower, K.N., Boudries, H., Canagaratna, M.R., Jimenez, J.L., Jayne, J.T., Garforth, A.A., Li, S.M., Worsnop, D.R.: Characterization of urban and rural organic particulate in the lower Fraser valley using two aerodyne aerosol mass spectrometers, *Atmospheric Environment*, 38, 34, 5745-5758, 2004.

Allan, J.D., Delia, A.E., Coe, H., Bower, K.N., Alfarra, M.R., Jimenez, J.L., Middlebrook, A.M., Drewnick, F., Onasch, T.B., Canagaratna, M.R., Jayne, J.T., Worsnop, D.R.: A generalised method for the extraction of chemically resolved mass spectra from aerodyne aerosol mass spectrometer data, *Journal of Aerosol Science*, 35, 7, 909-922, 2004.

Cofer, W.R., Collins, V.G., Talbot, R.W.: Improved aqueous scrubber for collection of soluble atmospheric trace gases, *Environ. Sci. Technol.*, 19, 557-560, 1985.

DeCarlo, P.F., Dunlea, E.J., Kimmel, J.R., Aiken, A.C., Sueper, D., Crounse, J., Wennberg, P.O., Emmons, L., Shinozuka, Y., Clarke, A., Zhou, J., Tomlinson, J., Collins, D., Knapp, D., Weinheimer, A., Campos, T., Jimenez, J.L.: Fast Airborne Aerosol Size and Chemistry Measurements with the High Resolution Aerosol Mass Spectrometer During the MILAGRO Campaign, *Atmos. Chem. Phys.*, 8, 4027–4048, 2008.

Herndon, S.C., Onasch, T.B., Wood, E.C., Kroll, J.H., Canagaratna, M.R., Jayne, J.T., Zavala, M.A., Knighton, W.B., Mazzoleni, C., Dubey, M.K., Ulbrich, I.M., Jimenez, J.L., Seila, R., Gouw, J.A.d., Foy, B.d., Fast, J., Molina, L.T., Kolb, C.E., Worsnop, D.R.: The Correlation of Secondary Organic Aerosol with Odd Oxygen in a Megacity Outflow, *Geophys. Res. Lett.*, 35, L15804, doi:10.1029/2008GL034058, 2008.

Jimenez, J.L., Jayne, J.T., Shi, Q., Kolb, C.E., Worsnop, D.R., Yourshaw, I., Seinfeld, J.H., Flagan, R.C., Zhang, X., Smith, K.A., Morris, J., Davidovits, P.: Ambient Aerosol Sampling Using the Aerodyne Aerosol Mass Spectrometer, *Journal of Geophysical Research*, 108, D7, 8425, doi:10.1029/2001JD001213, 2003.

Kondo, Y., Morino, Y., Fukuda, M., Kanaya, Y., Miyazaki, Y., Takegawa, N., Tanimoto, H., McKenzie, R., Johnston, P., Blake, D.R., Murayama, T., Koike, M.: Formation and transport of oxidized reactive nitrogen, ozone, and secondary organic aerosol in Tokyo, *J. Geophys. Res.*, 113, D21310, doi:10.1029/2008JD010134, 2008.

Mohr, C., Huffman, J.A., Cubison, M.J., Aiken, A.C., Docherty, K.S., Kimmel, J.R., Ulbrich, I.M., Hannigan, M., Jimenez, J.L.: Characterization of Primary Organic Aerosol Emissions from Meat Cooking, Trash Burning, and Motor Vehicles with High-Resolution Aerosol Mass Spectrometry and Comparison with Ambient and Chamber Observations, *Env. Sci. and Tech.*, 43, 7, 2443-2449, 2009.

Zhang, Q., Alfarra, M.R., Worsnop, D.R., Allan, J.D., Coe, H., Canagaratna, M.R., Jimenez, J.L.: Deconvolution and quantification of hydrocarbon-like and oxygenated organic aerosols based on aerosol mass spectrometry, *Environmental Science & Technology*, 39, 13, 4938-4952, 2005a.

Zhang, Q., Canagaratna, M.R., Jayne, J.T., Worsnop, D.R., Jimenez, J.L.: Time- and size-resolved chemical composition of submicron particles in Pittsburgh: Implications for aerosol sources and processes, *Journal of Geophysical Research-Atmospheres*, 110, D7, 19, D07S09, doi:10.1029/2004JD004649, 2005b.
Zhang, Q., Jimenez, J.L., Canagaratna, M.R., Allan, J.D., Coe, H., Ulbrich, I., Alfarra, M.R., Takami, A., Middlebrook, A.M., Sun, Y.L., Dzepina, K., Dunlea, E., Docherty, K., DeCarlo, P.F., Salcedo, D., Onasch, T., Jayne, J.T., Miyoshi, T., Shimono, A., Hatakeyama, S., Takegawa, N., Kondo, Y., Schneider, J., Drewnick, F., Weimer, S., Demerjian, K., Williams, P., Bower, K., Bahreini, R., Cotrell, L., Griffin, R., Rautiainen, J., Worsnop, D.R.: Ubiquity and Dominance of Oxygenated Species in Organic Aerosols in Anthropogenically—Influenced Northern Hemisphere Mid-latitudes, *Geophysical Research Letters*, 34, L13801, doi:10.1029/2007GL029979, 2007.
Zhang, Q., Stanier, C.O., Canagaratna, M.R., Jayne, J.T., Worsnop, D.R., Pandis, S.N., Jimenez, J.L.: Insights into the chemistry of new particle formation and growth events in Pittsburgh based on aerosol mass spectrometry, *Environmental Science & Technology*, 38, 18, 4797-4809, 2004.
Zhang, Q., Worsnop, D.R., Canagaratna, M.R., Jimenez, J.L.: Hydrocarbon-like and oxygenated organic aerosols in Pittsburgh: insights into sources and processes of organic aerosols, *Atmospheric Chemistry and Physics*, 5, 3289-3311, 2005c.